Predictions of heavy-flavor suppression at 5.1 TeV Pb + Pb collisions at the CERN Large Hadron Collider

Magdalena Djordjevic
Institute of Physics Belgrade, University of Belgrade, Serbia

Marko Djordjevic
Faculty of Biology, University of Belgrade, Serbia

(Received 20 May 2015; revised manuscript received 17 July 2015; published 28 August 2015)

High momentum hadron suppression is considered to be an excellent probe of jet-medium interactions in QCD matter created in ultrarelativistic heavy ion collisions. We previously showed that our dynamical energy loss formalism can accurately explain suppression measurements at 200 GeV Au + Au collisions at the Relativistic Heavy Ion Collider (RHIC) and 2.76 TeV Pb + Pb collisions at the CERN Large Hadron Collider (LHC). With the upcoming LHC measurements at notably higher collision energies, there is a question of what differences, with respect to the current (2.76 TeV) measurements, can be expected. In this paper we concentrate on heavy flavor suppression at the upcoming 5.1 TeV Pb + Pb collisions energy at the LHC. Naively, one would expect a notably ($\sim$30%) larger suppression at 5.1 TeV collision energy, due to estimated (significant) energy loss increase when transitioning from 2.76 to 5.1 TeV. Surprisingly, more detailed calculations predict nearly the same suppression results at these two energies. We show that this unexpected result is due to an interplay of the following two effects, which essentially cancel each other: (i) flattening of the initial charm and bottom momentum distributions with increasing collision energies, and (ii) significantly slower than naively expected increase in the energy loss. Therefore, the obtained theoretical predictions, which suggest nearly the same heavy flavor suppression at 2.76 and 5.1 TeV, provide a clear (qualitative and quantitative) test of our energy loss formalism.

DOI: 10.1103/PhysRevC.92.024918 PACS number(s): 12.38.Mh, 24.85.+p, 25.75.−q

I. INTRODUCTION

High energy heavy flavor suppression is considered to be an excellent probe of QCD matter created in ultra-relativistic heavy ion collisions at the Relativistic Heavy Ion Collider (RHIC) and the CERN Large Hadron Collider (LHC) [1–3]. One of the major goals of these experiments is mapping the quark-gluon plasma (QGP) properties [4–6], which requires comparing available suppression data with the theoretical predictions [7–9]. Such comparison tests different theoretical models and provides an insight into the underlying QGP physics [10–13]. Having this in mind, the upcoming 5.1 TeV Pb + Pb measurements at LHC (expected at the end of 2015)—and their comparison with theoretical predictions—will provide an additional important insight into the jet-medium interactions in QGP created in such collisions [14,15]. Motivated by this, the goal of this paper is providing the heavy flavor suppression predictions, and physical interpretation behind the obtained results, for the upcoming high-luminosity experimental data at 5.1 TeV Pb + Pb collisions at LHC. In particular, we aim to assess the differences in the predicted suppression with respect to the already available 2.76 TeV measurements [16,17] at LHC and compare the results of state-of-the-art calculations with simple expectations and estimates.

To generate the theoretical predictions we will use our recently developed dynamical energy loss formalism, which includes (i) dynamical scattering centers, (ii) QCD medium of a finite size [18], (iii) both radiative [18] and collisional [19] energy losses, (iv) finite magnetic mass effects [20], and (v) running coupling [21]. This energy loss formalism is based on the pQCD calculations in a finite size optically thin dynamical QCD medium, and has been incorporated into a numerical procedure [21] that allows generating state-of-the art suppression predictions. The model has shown to be successful in explaining a wide range of angular averaged observables [21,22] at both RHIC and LHC. Since it was previously shown [23–25] that the *angular averaged* R_{AA} is only weakly sensitive to the medium evolution, this observable can be considered as an excellent probe for jet-medium interactions, as it does not depend on the details of medium evolution; note that this is in distinction to differential R_{AA} observables (e.g., elliptic flow), which are likely highly sensitive to the medium evolution and are therefore commonly used as probes [26] for the bulk properties of the medium.[1] Consequently, the suppression predictions at 5.1 TeV Pb + Pb collisions at LHC, and their comparison with the measurements, will allow further testing of our energy loss formalism.

II. OVERVIEW OF THE COMPUTATIONAL FRAMEWORK

For generating the suppression predictions, we use the computational procedure from [21]. The main features are briefly summarized below, while the full account of the procedure is provided in [21].

[1]Note that explicitly testing these findings within our dynamical energy loss formalism, i.e., the importance of transverse and longitudinal medium expansion on both angular average R_{AA} and elliptic flow, is our future goal.

The quenched spectra of heavy flavor observables are calculated according to the generic pQCD convolution:

$$\frac{E_f d^3\sigma}{dp_f^3} = \frac{E_i d^3\sigma(Q)}{dp_i^3} \otimes P(E_i \to E_f) \otimes D(Q \to H_Q) \otimes f(H_Q \to e, J/\psi). \quad (1)$$

In the equation above, subscripts i and f correspond, respectively, to "initial" and "final," and Q denotes heavy quarks. $E_i d^3\sigma(Q)/dp_i^3$ denotes the initial heavy quark spectrum, which is computed at next-to-leading order according to [27,28]. $P(E_i \to E_f)$ is the energy loss probability; this probability includes both radiative and collisional energy loss in a finite size dynamical QCD medium, multigluon [29] and path-length fluctuations [30], and running coupling [21]. $D(Q \to H_Q)$ is the fragmentation function of heavy quark Q to hadron H_Q, where for D and B mesons we use BCFY [31] and KLP [32] fragmentation functions, respectively. Finally, decay of B mesons to experimentally measured nonprompt J/ψ is represented by $f(H_Q \to J/\psi)$ and obtained according to [27].

The expression for the radiative energy loss in a finite size dynamical QCD medium is extracted from Eq. (10) in [20], while the collisional energy loss is extracted from Eq. (14) in [19]. Path length distributions are taken from [33].

The angular averaged R_{AA} is a clear jet-medium interaction probe, i.e., it was previously shown [23–25] that it is largely insensitive to the details of the medium evolution. We therefore model the medium by assuming a constant average temperature of QGP. To determine the average temperatures at 0–10% most central collisions, we start from $T = 304$ MeV (the effective temperature extracted by ALICE [34] for 0–40% centrality), and use the procedure outlined in [22] (based on gluon rapidity density) to determine the temperatures at central collisions at 2.76 and 5.1 TeV Pb + Pb collisions; for 2.76 TeV 0–10% centrality, this leads to the average temperature of 313 MeV. To determine the temperature at 5.1 TeV, note that it is expected that the gluon rapidity density will be 25% higher at 5.1 TeV than at 2.76 TeV in Pb + Pb collisions at LHC [35]. Since the temperature is proportional to the gluon rapidity density, i.e., $T \sim (dN_g/dy)^{1/3}$, this leads to ~7% higher temperature at 5.1 TeV compared to 2.76 TeV at the LHC, i.e., 335 MeV for 0–10% central 5.1 TeV Pb + Pb collisions at LHC. Note that, in our energy loss calculations, this is the only parameter that differs between the two systems; i.e., all the other parameters that enter in the calculations (stated in the next paragraph) are the same, and correspond to the standard literature values (i.e., there are no free parameters determined through fitting the data).

The following parameters are used in the numerical calculations: QGP with effective light quark flavors $n_f = 3$ and perturbative QCD scale of $\Lambda_{QCD} = 0.2$ GeV. The Debye mass is taken to be $\mu_E \approx 0.9$ ($\mu_E \approx 0.97$) GeV for 2.76 (5.1) TeV collision energy, and is obtained by self-consistently solving Eq. (7) in [36]. The value for magnetic to electric mass ratio μ_M/μ_E is extracted from non-perturbative calculations [37–40] $0.4 < \mu_M/\mu_E < 0.6$; the gluon mass is $m_g = \mu_E/\sqrt{2}$ [41], while the charm and the bottom masses are, respectively, $M = 1.2$ GeV and $M = 4.75$ GeV. Path-length distribution, parton production, fragmentation functions, and decays, which are used in the numerical calculations, are specified above.

III. RESULTS AND DISCUSSION

To get a rough insight of what results we expect at 5.1 TeV collisions at the LHC, we will first provide a simple (commonly used) analytic estimate for heavy flavor suppression at this collision energy. For that purpose, note that radiative energy loss is widely considered to be a dominant energy loss mechanism in QGP (see, e.g., [42,43]), so, for simplicity, we will use only the radiative contribution for the estimate. Since it is also widely assumed that radiative energy loss is proportional to T^3 (see, e.g., [44]), one can estimate that the energy loss at 5.1 TeV should be ~25% higher than at 2.76 TeV. Based on this, and if we assume that initial momentum distributions can be approximated by power law distributions [29], i.e., $d\sigma/dp_\perp^2 \sim 1/p_\perp^n$, we can estimate how much largeror smaller suppression one would expect at 5.1 TeV compared to the already observed results at 2.76 TeV.

It was previously shown that, for radiative energy loss and power law initial momentum distributions, suppression can be roughly estimated by using the following simple formula[2] [29]:

$$\left(1 - \frac{1}{2}\frac{\Delta E}{E}\right)^{(n-2)} \approx \left(1 - \frac{n-2}{2}\frac{\Delta E}{E}\right), \quad (2)$$

where $\Delta E/E$ is the fractional energy loss. If we assume that, at 2.76 TeV, typical fractional energy loss for charm is ~30% and for bottom ~15%, and that charm and bottom initial momentum distributions do not notably change between these two collision energies, with $n \sim 6.5$ ($n \sim 6$) for charm (bottom), the above estimate will straightforwardly lead to the expectation of ~30% (~10%) larger suppression for charm (bottom) at 5.1 TeV compared to 2.76 TeV Pb + Pb collisions at the LHC.

Contrary to these expectations, Fig. 1 shows that our suppression calculations—obtained from the energy loss formalism outlined in the previous section—provide substantially different predictions. From this figure, we actually do not observe any suppression increase between 2.76 to 5.1 TeV collisions at the LHC. That is, we obtain the same suppression patterns for both charm and bottom probes (D mesons and nonprompt J/ψ) at these two collision energies. This then leads to the question of why the increase in the collision energy by almost a factor of 2 leads to the same predicted suppression patterns between the two collisional energies, despite the estimated significant (i.e., ~30% for charm, see above) increase in the suppression.

To address this question, in Fig. 2 we first compare charm and bottom initial momentum distributions between these two collision energies. From this figure, we see that the distributions at 5.1 TeV are slightly flatter than at 2.76 TeV,

[2]This formula should not be used for reliable predictions; we here use it only for the purpose of an analytical estimate.

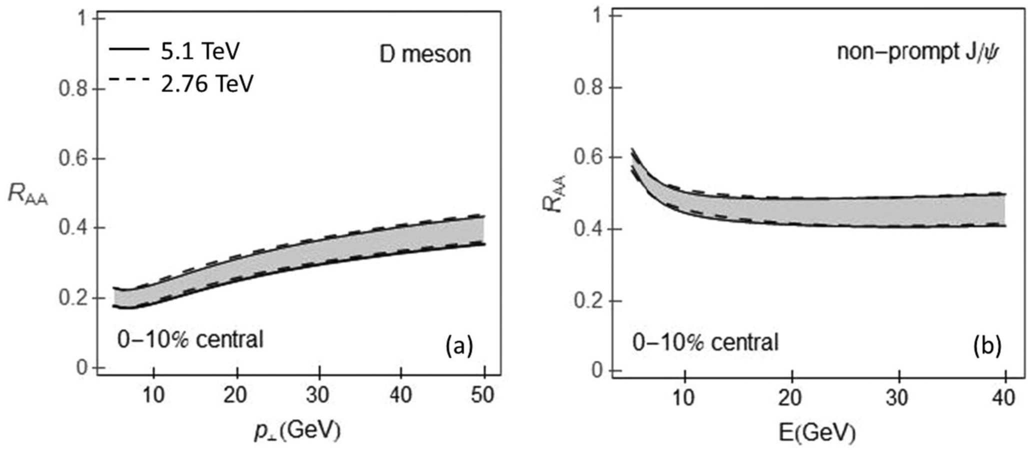

FIG. 1. Comparison of R_{AA} predictions for heavy flavor at 2.76 and 5.1 TeV. D mesons and nonprompt J/ψ suppression predictions, as a function of transverse momentum, are shown in panels (a) and (b), respectively. Full (dashed) curves correspond to R_{AA} predictions at 5.1 TeV (2.76 TeV) Pb + Pb collisions at the LHC. In each panel, the gray bands correspond to the finite magnetic mass case (i.e., $0.4 < \mu_M/\mu_E < 0.6$ [37–40]), where the lower and the upper boundaries correspond, respectively, to $\mu_M/\mu_E = 0.4$ and $\mu_M/\mu_E = 0.6$.

for both charm and bottom, which will have the tendency to somewhat lower the suppression at 5.1 TeV compared to 2.76 TeV. Note that only the shape of the distributions contributes to the suppression predictions, and from Fig. 2 one can observe that the differences in the shape of the distributions are not large. Still, this difference in the distributions has a notable (though again not large, i.e., ∼5%) effect on the suppression predictions, as can be seen in panel (a) of Fig. 3; therefore, it should be taken into account in the suppression calculations.

However, what we further see from panel (b) of Fig. 3 is that the effect on the suppression coming from the energy loss increase between 2.76 and 5.1 TeV (due to the increase in average temperature) is also notable but not large, i.e., it corresponds to ∼5 and 10% for bottom and charm quarks, respectively. That is, the energy loss effect on the suppression has about the same magnitude, but an opposite direction, compared to the effect of different initial momentum distributions between these two collision energies.[3] The first question that we want to address is why the effect of the energy loss increase on jet suppression is not larger between these two collision energies, at least not for the charm quark. That is, based on the common T^3 assumption, we have estimated that the energy loss increase should be on the order of 25%, which should, therefore, have a more prominent (estimated 30%) effect on the suppression.

Regarding the T^3 estimate for the radiative energy loss, note that, while widely used, this estimate does not have to

[3]For the bottom quark, these two effects indeed almost perfectly cancel each other, as shown in Fig. 3. For the charm quark, the energy loss effect is somewhat larger than the effect of different initial momentum distributions, and it therefore leads to the expectation of slightly larger [though likely experimentally not noticeable, see panel (a) in Fig. 1] suppression at 5.1 TeV compared to 2.76 TeV collision energy.

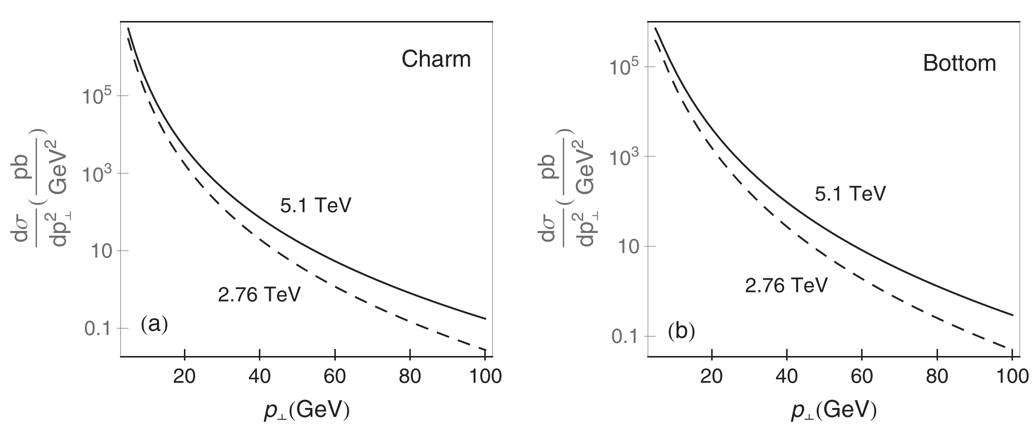

FIG. 2. Comparison of initial momentum distributions for charm and bottom at 2.76 and 5.1 TeV. Charm and bottom initial momentum distributions, as a function of transverse momentum, are shown in panels (a) and (b), respectively. In each panel, the full (dashed) curve corresponds to the momentum distribution at 5.1 TeV (2.76 TeV) Pb + Pb collisions at the LHC.

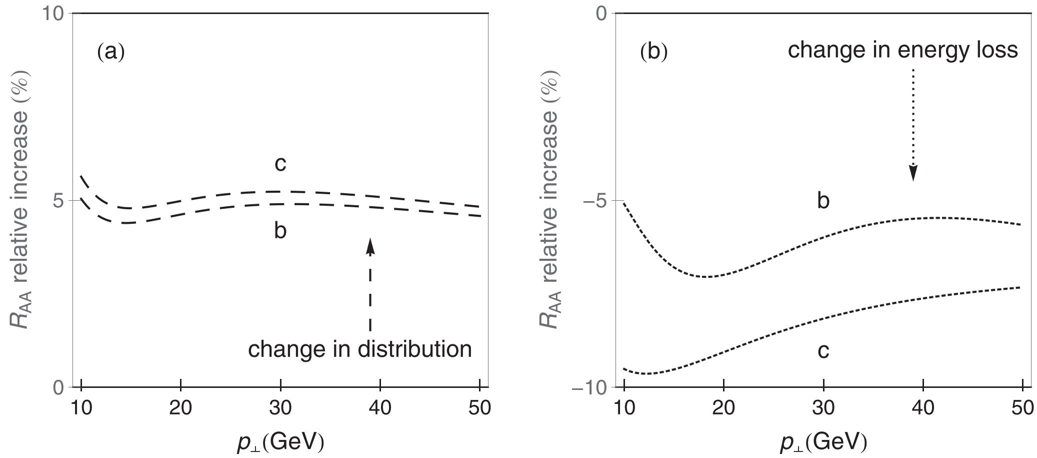

FIG. 3. Relative increase in R_{AA} between 2.76 and 5.1 TeV. Panel (a) shows momentum dependence of the relative increase in R_{AA} between 2.76 and 5.1 TeV Pb + Pb collisions at the LHC due to differences in the initial momentum distributions; to calculate the relative increase in R_{AA} due to different initial momentum distributions, the energy loss is kept fixed and calculated for the 2.76 TeV case, while the distributions are varied between 2.76 and 5.1 TeV. Panel (b) shows momentum dependence of the relative increase in R_{AA} between 2.76 and 5.1 TeV collisions at the LHC due to differences in the energy loss; to calculate the relative increase in R_{AA} due to different energy losses, the initial momentum distribution is kept fixed and calculated for the 2.76 TeV case, while the energy loss is varied between 2.76 and 5.1 TeV. In each panel, curves that correspond to charm and bottom are marked by c and b, respectively, and the magnetic mass is fixed to $\mu_M/\mu_E = 0.4$.

be realistic. That is, from Eq. (10) in [20], which shows the radiative energy loss expression in a finite size dynamical QCD medium, it can be straightforwardly observed that the expression nontrivially depends on T and that its dependence cannot be analytically determined. That is, while one can recover a part with explicit dependence on T^3 in this expression, the rest of the expression depends nontrivially on T, where this extra (*multiplicative*) term can considerably modify the temperature dependence. Additionally, the collisional energy loss effect, while smaller compared to the radiative, is still important, and this effect also has to be taken into account in the suppression calculations. Note that, for the collisional energy loss, it is commonly assumed that it has a quadratic (T^2) dependence on the temperature. However, similarly to the above discussion for the radiative energy loss, Eq. (14) from [19] shows a nontrivial temperature dependence, so we will below also numerically test whether this simple (T^2) assumption is justified.

With these goals, in Fig. 4, we plot the relative heavy flavor energy loss increase between 2.76 and 5.1 collision energies at the LHC. Figures also contain dashed horizontal lines, which represent what would be the energy loss increase if it would indeed have T^2 or T^3 dependence. For radiative energy loss, we see that, contrary to the common expectations, energy loss increase is far from T^3 dependence; i.e., it is between linear (for low jet energy regions) and quadratic (which can be reached for asymptotically high jet energies). Consequently, for the high momentum heavy flavor hadrons that will be studied at these two collision energies at the LHC, the expected energy loss increase is notably smaller than quadratic, i.e. it is in the region of 5–10% (note that the average temperature

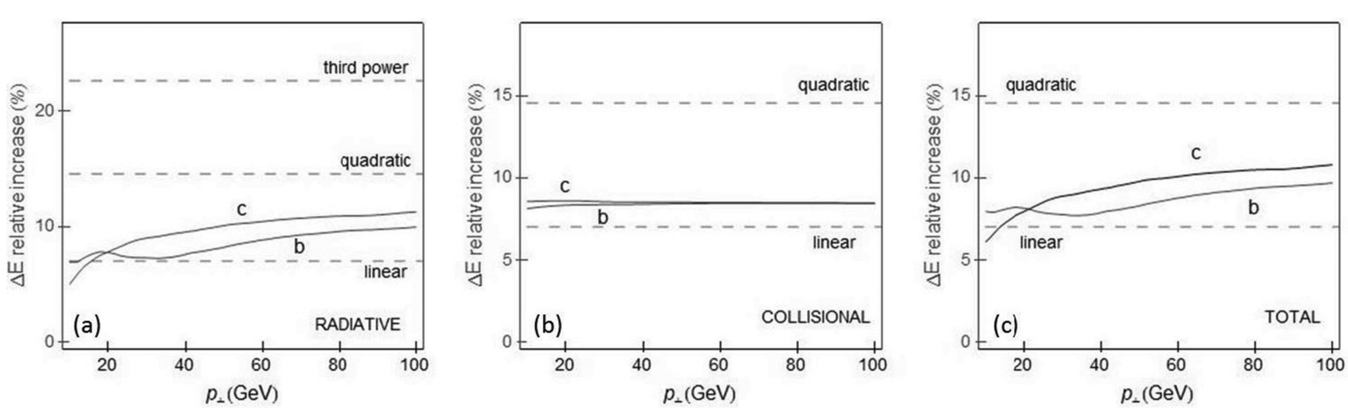

FIG. 4. Relative energy loss increase between 2.76 and 5.1 TeV. All the panels show the momentum dependence of the relative energy loss increase between 5.1 and 2.76 TeV Pb + Pb collisions at the LHC. Panels (a), (b), and (c) correspond, respectively, to the radiative, collisional, and total energy loss cases. In each panel curves that correspond to charm (bottom) are marked by letter c (b) and the magnetic mass is fixed to $\mu_M/\mu_E = 0.4$. Dashed gray horizontal lines represent the energy loss increase if it would have linear, quadratic, or cubic temperature dependence.

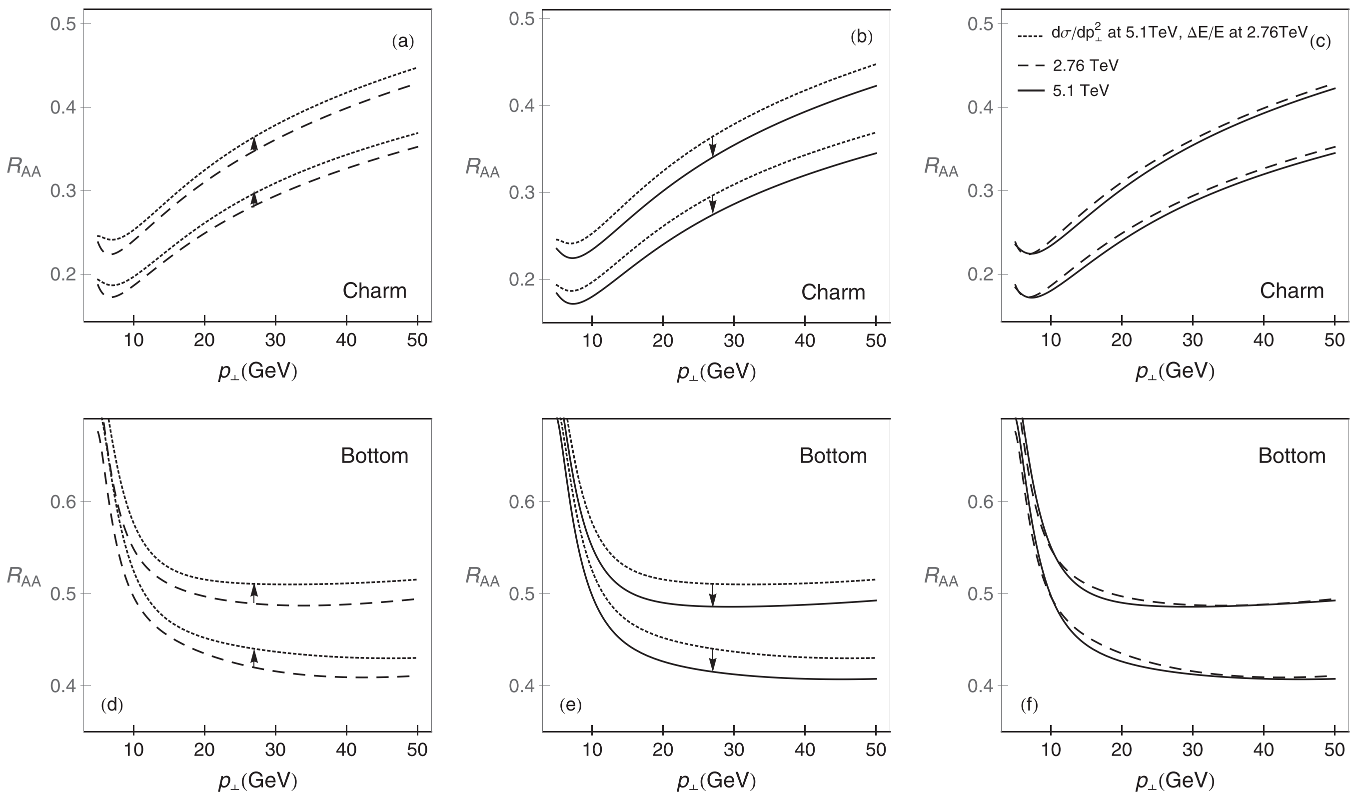

FIG. 5. Analysis of the heavy flavor suppression between 2.76 and 5.1 TeV. The full curves correspond to R_{AA}s with both the energy losses and the initial momentum distributions calculated at 5.1 TeV collision energy. The dashed curves correspond to R_{AA}s with both the energy losses and the initial momentum distributions calculated at 2.76 TeV collision energy. The dotted curves correspond to R_{AA}s where the energy losses are calculated at 2.76 TeV collision energy, while the distributions are calculated at 5.1 TeV collision energy. The upper (lower) panels correspond to the charm (bottom) quark. The left panels [(a) and (d)] show how the flatter distributions at 5.1 TeV lower the heavy flavor suppression compared to the 2.76 TeV case. The central panels [(b) and (e)] show how increase in the energy loss at 5.1 TeV increases the suppression compared to the 2.76 TeV case. The right panels [(c) and (f)] show how the above two effects cancel, so as to reproduce almost the same suppression at 2.76 and 5.1 TeV Pb + Pb collision energy. In each panel, lower (upper) set of curves corresponds to the magnetic-to-electric mass ratio of $\mu_M/\mu_E = 0.4$ ($\mu_M/\mu_E = 0.6$).

increase between these two collision energies is ∼7%). For the collisional energy loss, we also see that the energy loss increase is far from quadratic; i.e., the increase of ∼8.5% is constant with momentum and it has slightly larger than linear dependence on temperature. Consequently, contrary to the common expectation, the total energy loss has also a modest increase with temperature, which is close to linear, i.e., 6–10% depending on the jet momentum. This modest energy loss increase between the two collisional energies consequently leads to a modest increase in the suppression, which we observe in panel (b) of Fig. 3.

Finally, in Fig. 5, we study the combined effect of the differences in the initial momentum distributions and the energy loss on jet suppression. In the two left panels [(a) and (d)], we see the effect of the difference in the initial momentum distributions on the jet suppression, while the energy loss is kept fixed. In the two central panels [(b) and (e)], we keep the same distribution but change the energy loss, while in the two right panels [(c) and (f) both the distributions and the energy loss are changed between the two collision energies. From the panels, we see that, while the change in the initial momentum distribution has the tendency to reduce the suppression, the energy loss increase increases the suppression by about the same amount, so that the resultant suppression at 5.1 TeV collision energy is almost the same as at 2.76 TeV. Note that this is the main result of our paper, which is in fact quite robust with the uncertainties in the value of the average temperature of the medium, as both of the suppressions (at 2.76 and 5.1 TeV) would shift in the same direction and amount with the variations in temperature, therefore not changing the overlap in the two suppressions. Moreover, our R_{AA} results are linearly dependent on the average temperature, so even their absolute (i.e., not only the relative) values will not significantly change with the reasonable magnitude of the temperature uncertainty.

The above obtained numerical result can also be directly estimated from Eq. (2). For this purpose, we will take that the energy loss between 2.76 and 5.1 TeV collision energy increases by a factor η, where from Fig. 4 we see that $\eta \approx 10\%$ for both charm and bottom. Additionally, we will take that the power factors in the initial momentum distributions decrease by δ; by fitting the power law to the ratio of the initial momentum distributions in Fig. 2, we obtain $\delta \approx 0.4$. By applying these factors to Eq. (2), one can straightforwardly obtain

$$R_{AA}(5.1\text{ TeV}) \approx R_{AA}(2.76\text{ TeV}) + \frac{1}{2}\frac{\Delta E}{E}[\delta - \eta(n-2)], \tag{3}$$

where for δ and η estimated above the second term in the above expression approaches zero. Consequently, this estimate also recovers the conclusion of the same heavy flavor suppression at 2.76 and 5.1 TeV Pb + Pb collision energies at the LHC.

IV. CONCLUSION

In this paper, we provided heavy flavor suppression predictions for the upcoming 5.1 TeV Pb + Pb collisions at the LHC. Based on our energy loss formalism, we predict the same heavy flavor suppression for 2.76 and 5.1 TeV collision energies. This result is surprising since, based on the commonly used assumption, a notable increase of the suppression is expected at the higher collision energy. We showed that the same suppression is a consequence of the interplay between the following two effects: (i) a decrease in the suppression due to flattening of the initial momentum distributions, and (ii) an increase in the suppression—though more moderate than naively expected—due to higher energy loss. Consequently, this unexpected but simple suppression prediction provides a direct (both quantitative and qualitative) test of our understanding of the medium interactions in QCD medium created in these collisions.

ACKNOWLEDGMENTS

This work is supported by Marie Curie International Reintegration Grant within the 7th European Community Framework Programme PIRG08-GA-2010-276913 and by the Ministry of Science and Technological Development of the Republic of Serbia, under Projects No. ON171004 and No. ON173052.

[1] J. D. Bjorken, Fermilab Report No. FERMILAB-PUB-82-059-THY, 1982 (unpublished), pp. 287–292.
[2] X. N. Wang, Nucl. Phys. A **932**, 1 (2014).
[3] T. Song *et al.*, Phys. Rev. C **92**, 014910 (2015).
[4] U. Heinz *et al.*, arXiv:1501.06477.
[5] Y. Akiba *et al.*, arXiv:1502.02730.
[6] B. Muller, Nucl. Phys. A **910-911**, 5 (2013).
[7] N. Brambilla *et al.*, Eur. Phys. J. C **74**, 2981 (2014).
[8] M. Gyulassy, in *Lectures on Quark Matter*, Lecture Notes in Physics Vol. 583 (Springer, Berlin, 2002), p. 37.
[9] D. d'Enterria and B. Betz, in *The Physics of the Quark-Gluon Plasma*, Lecture Notes in Physics Vol. 785 (Springer, Berlin, 2010), p. 285.
[10] M. Gyulassy and L. McLerran, Nucl. Phys. A **750**, 30 (2005).
[11] B. Jacak and P. Steinberg, Phys. Today **63**(5), 39 (2010).
[12] E. Shuryak, arXiv:1412.8393.
[13] K. M. Burke *et al.*, Phys. Rev. C **90**, 014909 (2014).
[14] F. Antinori *et al.*, arXiv:1409.2981.
[15] A. Andronic *et al.*, arXiv:1506.03981.
[16] A. Grelli (for the ALICE collaboration), Nucl. Phys. A **904-905**, 635c (2013); S. Sakai (for the ALICE collaboration), *ibid.* **904-905**, 661c (2013).
[17] J. Mihee (for the CMS collaboration), Nucl. Phys. A **904-905**, 657c (2013); CMS Collaboration, CMS Report No. PAS HIN-12-014, 2012 (unpublished).
[18] M. Djordjevic, Phys. Rev. C **80**, 064909 (2009).
[19] M. Djordjevic, Phys. Rev. C **74**, 064907 (2006).
[20] M. Djordjevic and M. Djordjevic, Phys. Lett. B **709**, 229 (2012).
[21] M. Djordjevic and M. Djordjevic, Phys. Lett. B **734**, 286 (2014).
[22] M. Djordjevic, M. Djordjevic, and B. Blagojevic, Phys. Lett. B **737**, 298 (2014).
[23] D. Molnar and D. Sun, Nucl. Phys. A **932**, 140 (2014); **910-911**, 486 (2013).
[24] T. Renk, Phys. Rev. C **85**, 044903 (2012).
[25] T. Renk, J. Ruppert, C. Nonaka, and S. A. Bass, Phys. Rev. C **75**, 031902(R) (2007).
[26] U. Heinz and R. Snellings, Annu. Rev. Nucl. Part. Sci. **63**, 123 (2013).
[27] M. Cacciari, S. Frixione, N. Houdeau, M. L. Mangano, P. Nason, and G. Ridolfi, J. High Energy Phys. 10 (2012) 137.
[28] M. Cacciari, M. Greco, and P. Nason, J. High Energy Phys. 05 (1998) 007; M. Cacciari, S. Frixione, and P. Nason, *ibid.* 03 (2001) 006.
[29] M. Gyulassy, P. Levai, and I. Vitev, Phys. Lett. B **538**, 282 (2002).
[30] S. Wicks, W. Horowitz, M. Djordjevic, and M. Gyulassy, Nucl. Phys. A **784**, 426 (2007).
[31] M. Cacciari and P. Nason, J. High Energy Phys. 09 (2003) 006; E. Braaten, K.-M. Cheung, S. Fleming, and T. C. Yuan, Phys. Rev. D **51**, 4819 (1995).
[32] V. G. Kartvelishvili, A. K. Likhoded, and V. A. Petrov, Phys. Lett. B **78**, 615 (1978).
[33] A. Dainese, Eur. Phys. J. C **33**, 495 (2004).
[34] M. Wilde (for the ALICE Collaboration), Nucl. Phys. A **904-905**, 573c (2013).
[35] K. Aamodt *et al.* (ALICE Collaboration), Phys. Rev. Lett. **105**, 252301 (2010).
[36] A. Peshier, arXiv:hep-ph/0601119.
[37] A. Nakamura, T. Saito, and S. Sakai, Phys. Rev. D **69**, 014506 (2004).
[38] A. Hart, M. Laine, and O. Philipsen, Nucl. Phys. B **586**, 443 (2000).
[39] D. Bak, A. Karch, and L. G. Yaffe, J. High Energy Phys. 08 (2007) 049.
[40] Yu. Maezawa *et al.* (WHOT-QCD Collaboration), PoS(LATTICE 2008)194.
[41] M. Djordjevic and M. Gyulassy, Phys. Rev. C **68**, 034914 (2003).
[42] N. Armesto, C. A. Salgado, and U. A. Wiedemann, Phys. Rev. D **69**, 114003 (2004).
[43] R. Baier, Y. Dokshitzer, A. Mueller, S. Peigne, and D. Schiff, Nucl. Phys. B **484**, 265 (1997); B. Zakharov, JETP Lett. **63**, 952 (1996); **65**, 615 (1997).
[44] B. Betz and M. Gyulassy, J. High Energy Phys. 08 (2014) 090; 10 (2014) 043.